INVESTIGATIONS INTO THE FEASIBILITY OF HIGH POWER LASER WINDOW MATERIALS

Jacob L. Zar

Avco Everett Research Laboratory

Prepared for:

Air Force Cambridge Research Laboratories
Defense Advanced Research Projects Agency

15 April 1975

AFCRL-TR-75-0264

INVESTIGATIONS INTO THE FEASIBILITY OF HIGH POWER LASER WINDOW MATERIALS

Jacob L. Zar
Avco Everett Research Laboratory, Inc.
2385 Revere Beach Parkway
Everett, MA. 02149

15 April 1975

Semiannual Technical Report No. 1

Sponsored by

DEFENSE ADVANCED RESEARCH PROJECTS AGENCY
ARPA Order No. 2806

AIR FORCE CAMBRIDGE RESEARCH LABORATORIES
AIR FORCE SYSTEMS COMMAND
UNITED STATES AIR FORCE
HANSCOM AFB, MASSACHUSETTS 01731

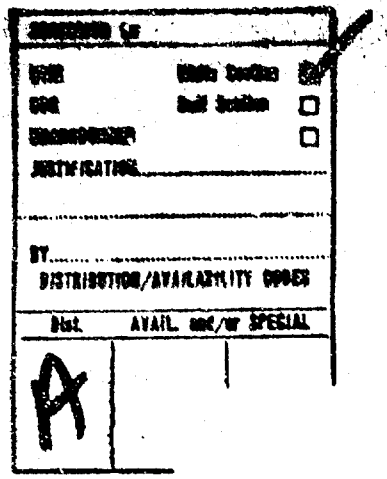

ARPA Order No: 2806

Program Code No: 5010

Name of Contractor: AERL, Inc.

Effective Date of Contract: 1-10-74

Contract No: F19628-75-C-0066

Principal Investigator and Phone No: Dr. J. L. Zar
(617) 389-3000, Ext. 225

AFCRL Project Scientist and Phone No: Major Charles V. Collins
(617) 861-4829

Contract Expiration Date: 30-9-76

Unclassified

SECURITY CLASSIFICATION OF THIS PAGE (When Data Entered)

REPORT DOCUMENTATION PAGE		READ INSTRUCTIONS BEFORE COMPLETING FORM
1. REPORT NUMBER AFCRL-TR-75-0264	2. GOVT ACCESSION NO.	3. RECIPIENT'S CATALOG NUMBER
4. TITLE (and Subtitle) INVESTIGATIONS INTO THE FEASIBILITY OF HIGH POWER LASER WINDOW MATERIALS		5. TYPE OF REPORT & PERIOD COVERED Scientific - Interim 6. PERFORMING ORG. REPORT NUMBER Semiannual Tech Rpt No. 1
7. AUTHOR(s) Jacob L. Zar		8. CONTRACT OR GRANT NUMBER(s) F19628-75-C-0066
9. PERFORMING ORGANIZATION NAME AND ADDRESS Avco Everett Research Laboratory, Inc. 2385 Revere Beach Parkway Everett, MA 02149		10. PROGRAM ELEMENT, PROJECT, TASK AREA & WORK UNIT NUMBERS 2806-n/a-n/a
11. CONTROLLING OFFICE NAME AND ADDRESS Air Force Cambridge Research Laboratories Hanscom AFB, Massachusetts 01731 Contract Monitor: Rudolf Bradbury/OPL		12. REPORT DATE 15 April 1975 13. NUMBER OF PAGES ~~36~~ 38
14. MONITORING AGENCY NAME & ADDRESS(if different from Controlling Office)		15. SECURITY CLASS. (of this report) Unclassified 15a. DECLASSIFICATION DOWNGRADING SCHEDULE

16. DISTRIBUTION STATEMENT (of this Report)

Approved for Public Release; Distribution Unlimited

DDC
DEC
JUL 14 1975
RECEIVED
D

17. DISTRIBUTION STATEMENT (of the abstract entered in Block 20, if different from Report)

18. SUPPLEMENTARY NOTES

This research was supported by the Defense Advanced Research Projects Agency, ARPA Order No. 2806

19. KEY WORDS (Continue on reverse side if necessary and identify by block number)

Laser Window Testing	CaF_2 Laser Window
Diamond Absorption Coefficient	Laser Window Stress
Type II Diamond Laser Windows	Laser Window Heating

20. ABSTRACT (Continue on reverse side if necessary and identify by block number)

A test facility is being constructed for testing laser window material. This will utilize the focused beam from a 15 kW CW laser at 10.6 μm or other available lasers. Provision for cooling the window is included and also instrumentation for measuring optical and mechanical effects.

Forty-seven natural diamonds have been tested to find the correlation between the UV absorption spectrum, the IR absorption spectrum and the absorption coefficient β at 10.6 μm. Transparency at .253 μm is roughly

DD FORM 1 JAN 73 1473 EDITION OF 1 NOV 65 IS OBSOLETE

Unclassified

SECURITY CLASSIFICATION OF THIS PAGE (When Data Entered)

correlated with low values of β. A water cooled diamond window holder is described.

A specimen of single crystal CaF_2 and another of pressure induced recrystalized CaF_2 were exposed to a 20 joule, 5μsec 6.7×10^7 watt/cm^2 pulse of 2.8μm laser radiation with no apparent damage.

TABLE OF CONTENTS

I. INTRODUCTION

The development of high power lasers has simultaneously generated a requirement for the development of windows capable of transmitting the laser beam from one environment to another without significant distortion of the wave front. At one time, the best available windows were aerodynamic windows. However, they are not suited to all interfaces. Therefore, an extensive program of material development was funded by the U. S. Government to develop solid state windows capable of transmitting high energy and high intensity laser beams for all useful wavelengths. These programs have born fruit in that there are now available improved window materials and coatings. It is reasonable now to propose to use solid state windows with all except the highest power lasers under development. There has arisen the need for a facility where windows may be tested for suitability for both pulsed and CW lasers.

This test facility should have the capability to measure changes in optical and mechanical properties of the window while transmitting the laser beam. For this, one needs access to high power pulsed and CW lasers, such as those available at the Avco Everett Research Laboratory, Inc. Therefore, an integrated research program has been authorized by the Advanced Projects Research Agency (ARPA) to be monitored by the Air Force Cambridge Research Laboratories (AFCRL) which calls for modification of an existing 10.6μ high power laser test facility for use with windows of various types. It will also be available under the authorization of our contract monitor to other laboratories who wish to test and evaluate their own materials.

One of the available lasers at Avco is the HPL* industrial laser. This can deliver a continuous beam of radiation at 10.6 μm with a power of about 15 kilowatts. A separate test station is being constructed for window testing. This is described in the next section. The experiment is mounted on a special moveable table so that it can be transferred to other lasers for testing at other wavelengths or with pulsed beams. One of the pulsed lasers is the 10.6 μm "breakdown" laser which can produce 80 J pulses of about 100 microseconds duration. When focused, it yields intensities approaching 10^9 W/cm^2. Other lasers with even shorter pulse lengths, higher power, or other wavelengths are available when scheduled.

Among the first materials to be tested at Avco will be diamonds. Some diamonds, called Type II are highly transparent to 10.6 μm radiation. These are considerably rarer than the Type I diamonds which are not as transparent at this wavelength. The problem is to select the Type II diamonds before embarking on the expense of cutting and polishing windows. The selection may be done by examining the infrared and ultraviolet absorption spectrum of the uncut stone. As will be shown later in this report, Type II diamonds are transparent at 7.9 μm and at 0.25 μm whereas Type I diamonds are not. The latter wavelength is easily obtained with a mercury arc. The diamond merchant can make a preliminary selection among his specimens by a simple photographic test. A description of this test is contained in the third section of this report. In the fourth section, some preliminary tests are described with CaF_2 windows exposed to a H-F pulsed laser. Finally, there is a discussion of the future plans for the window test facility.

---

* Trademark of AERL, Inc.

II. DESCRIPTION OF HPL INDUSTRIAL LASER TEST FACILITY

The laser is a closed cycle CO_2 machine producing a 10.6 μm beam of approximately 15 kW.[1] The output beam is collimated with a diameter of 3.8 cm and is transferred by mirrors and actuators to several work stations. Each work station may command the laser and has its own safety interlock system. When one is in use, the other stations may safely be entered for test preparation.

The laser power control has closed loop feedback. The power, its rate of rise and fall and the exposure time may all be varied by controlls at each test station.

The window test station is the third to be added to this laser. It is housed in a room about 6 ft sq having lucite panel walls. The experimentor may view the experiment and operate the laser from outside the room with complete safety.

The laser beam is brought to a sharp focus with an f/21 telescope. Diamonds and other small specimens may be put at the focus. For larger beams, the test specimen can be located off-focus. The laser mirrors and the holder for the test specimen are cooled by circulating water through a closed cycle heat exchanger. The water temperature is continuously maintained at 95°F and thus there is no condensation of moisture on the surfaces even on humid days. After passing through the test specimen, the beam is received in a calorimeter and the power measured. Alternatively, it may be absorbed in a beam dump. An exhaust is provided for removal of fumes generated either from the test specimen or from the beam dump.

---

(1) Hoag, E., Pease, H., Staal, S., and Zar, J., Performance Characteristics of a 10 kW Industrial CO_2 Laser System, Applied Optics 13, 1959, 1974.

The entire experiment is mounted on a sturdy optical table and maybe moved to other lasers if desired. In addition to water cooling, compressed gases are available for flushing the surface of test samples. These are controlled by a solenoid valve.

For instrumentation of the test, a second laser beam from a visible laser such as helium neon, is passed through the window at a small angle to the heating beam. The changes in the window that occur are observed by interference. The window is included in one leg of a Mach-Zehnder interferometer. A camera is used to photograph the interference patterns.

There is also available one or more thermocouples and a strip chart recorder for recording temperatures. Other types of instrumentation may be added as required by the experiment.

As of the date of this report, the test facility is being completed and it will shortly be calibrated for the available power, beam size and distribution.

III. DIAMOND SPECTRA

We have examined 47 natural diamonds to determine the infrared, the ultraviolet spectra and have measured the absorption coefficient for 10.6 μm radiation. The diamonds were in the shape of discs from 2 to 2.5 mm diameter by approximately 0.5 mm thick; clear natural stones.* The UV spectra were obtained with a Cary Model 1756 spectrometer and the infrared spectra with a Perkin Elmer Model 457 spectrometer. Because the diamonds were small, it was difficult to concentrate sufficient light intensity through them. Therefore, a Perkin Elmer 4X, All Reflecting Beam Condenser was used with the spectrometers and the instruments adjusted to give at least half scale deflection of the recorder by reducing the intensity of the reference light beam.

Figure 1 shows the ultraviolet spectra obtained with representative diamonds. These are shifted by an arbitrary amount along the vertical (intensity) scale so that they do not overlap. The number on the right is the identifying serial number of the diamond. It will become apparent from the measurement of β, the absorption coefficient at 10.6 μm described in the next section, that diamonds #13 and 28 have the lowest values of β. Diamonds #43 and 38 have much higher β's and the others fall in between. Figure 1 shows that diamonds with a high β (#43 and 38) also have a high absorption coefficient at .25 μm whereas diamonds with low β (#13 and 28) also have a low absorption at this wavelength. This figure further shows that the precise shape of the ultraviolet absorption edge is variable. For instance, diamonds 46 and 23 have very similar shaped absorption edges whereas we shall find a factor 3 difference in the values of β.

*These were kindly lent to us by Lazare Kaplan & Sons, Inc.

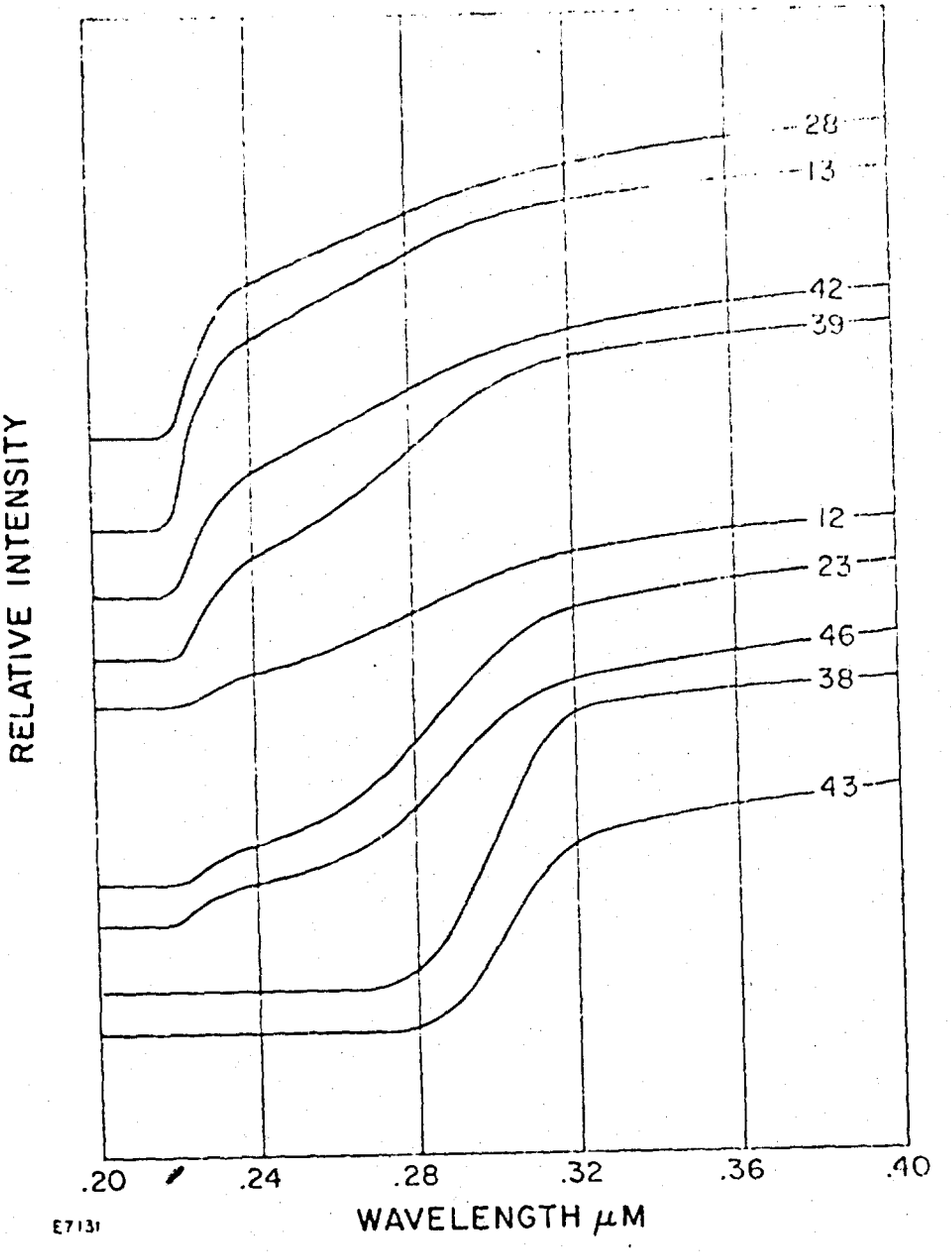

Figure 1. UV absorption spectrum of representative sample diamond discs.

It would be very useful if the transparency at .25 μm could be used as a basis for selection of the uncut stones. In order to characterize the spectrum by a single number, the following definition is used. The transmission at .25 μm, $I_{.25}$, is compared to the transmission at .40 μm, $I_{.40}$, measured with the spectrometer. The relative absorption at .25 μm is defined as

$$A_{.25} = 1 - (I_{.25}/I_{.40}) \quad (1)$$

Table I lists all of the data obtained for the 47 diamonds. The values of $A_{.25}$ are given in column 3.

In a similar way, the infrared absorption spectrum was obtained from 4.5 μm to 15 μm. These spectra are shown in Figure 2 for the same diamonds. Again, the curves are displaced along the intensity scale to prevent overlapping. (The discontinuity in the spectra at 5.0μm is due to automatic switching of the spectrometer optics which occurs at this wavelength.)

Some diamonds, notably numbers 13, 28, 42 and 39 show no significant absorption in the region from 7.5 to 8.5 μm. Others, notably numbers 38 and 43 show a very well pronounced absorption band and still others show varying amounts of absorption. This band has been attributed to interstitial nitrogen atoms lying in the (100) planes in concentrations up to several times 10^{20} atoms/cm^3.(2) The nitrogen impurity in natural diamonds reduces the thermal conductivity at low temperatures by about an order of magnitude, presumably by scattering of phonons. It also increases the indent hardness and reduces the plastic flow by interfering with the migration of dislocations. A pronounced absorption band at 8μm may also have a significant tail extending to 10.6 μm and thus increase β for the window at this wavelength.

---

(2) Strong, H. M. and Chrenko, R. M., Further Studies on Diamond Growth Rates and Physical Properties of Laboratory-Made Diamonds. J. Phys. Chem. 75 1838, 1971.

TABLE I DATA FOR DIAMOND SPECTRA AND ABSORPTION

Specimen No.	Thickness cm	$A_{.25}$	$A_{7.9}$	Exposure Time sec.	Incident Power watts	Transmitted Power watts	ΔT °C	Absorbed Power watts	Uncorrected β cm^{-1}	β cm^{-1}
1		.974	.321	*						
2		.914	.262	*						
3		.989	.384	*						
4	.048	.876	.408	10.3	33.1	17.4	62.6	1.37	.62	.81
5	.053	.885	.209	10.2	25.6	18.6	47.8	1.01	.76	.72
6		.980	.421	*						
7		.996	.458	*						
8		.996	.340	*						
9		1.000	.583	*						
10		1.000	.576	*						
11		.920	.277	*						
12	.060	.747	.102	15.1	32.2	19.9	37.2	0.58	.30	.31
13	.042	.480	.006	43.9	34.9	16.6	25.4	0.068	.045	.067
14		.925	.277	*						
15		.986	.310	*						
16		1.000	.900	Diamond turned black in a few seconds.						
17		.985	.407	*						
18		.998	.440	*						
19		.977	.326	*						
20	.036	.914	.259	15.1	29.8	18.0	49.3	.75	.71	.80
21		.961	.263	*						
22		1.000	.586	*						
23	.079	.830	.196	15.4	26.9	18.6	24.1	.32	.15	.16
24	.051	.938	.207	15.3	27.9	18.9	31.4	.46	.33	.35
25		1.000	.973	*						
26		.976	.336	*						
27		.986	.327	*						
28	.052	.446	.048	39.5	36.2	16.8	23.5	.028	.015	.021
29	.070	1.000	.624	15.2	24.1	16.5	123.0	2.07	1.28	1.23
30		.943	.273	*						
31	.053	.847	.113	24.9	32.3	17.9	47.3	.46	.27	.34
32		.988	.406	*						
33	.048	.863	.130	15.3	33.3	20.2	25.4	.35	.22	.27
34		1.000	.330	*						
35	.051	.857	.123	15.2	27.1	19.2	40.9	.63	.46	.45
36		.989	.406	*						
37		1.000	.442	*						
38	.039	1.000	.481	13.8	29.1	18.1	65.8	1.08	.97	1.07
39	.056	.636	.026	9.5	34.9	18.8	25.3	.46	.24	.30
40		.841	.154	*						
41		.990	.371	*						
42	.047	.526	.083	13.7	37.2	18.5	21.9	.26	.15	.21
43	.056	1.000	.633	8.0	25.0	15.9	99.5	2.56	1.92	1.95
44		.982	.391	*						
45		.979	.297	*						
46	.060	.813	.210	15.2	25.5	18.3	66.4	1.08	.72	.81
47		.846	.277	*						

* Not tested for β

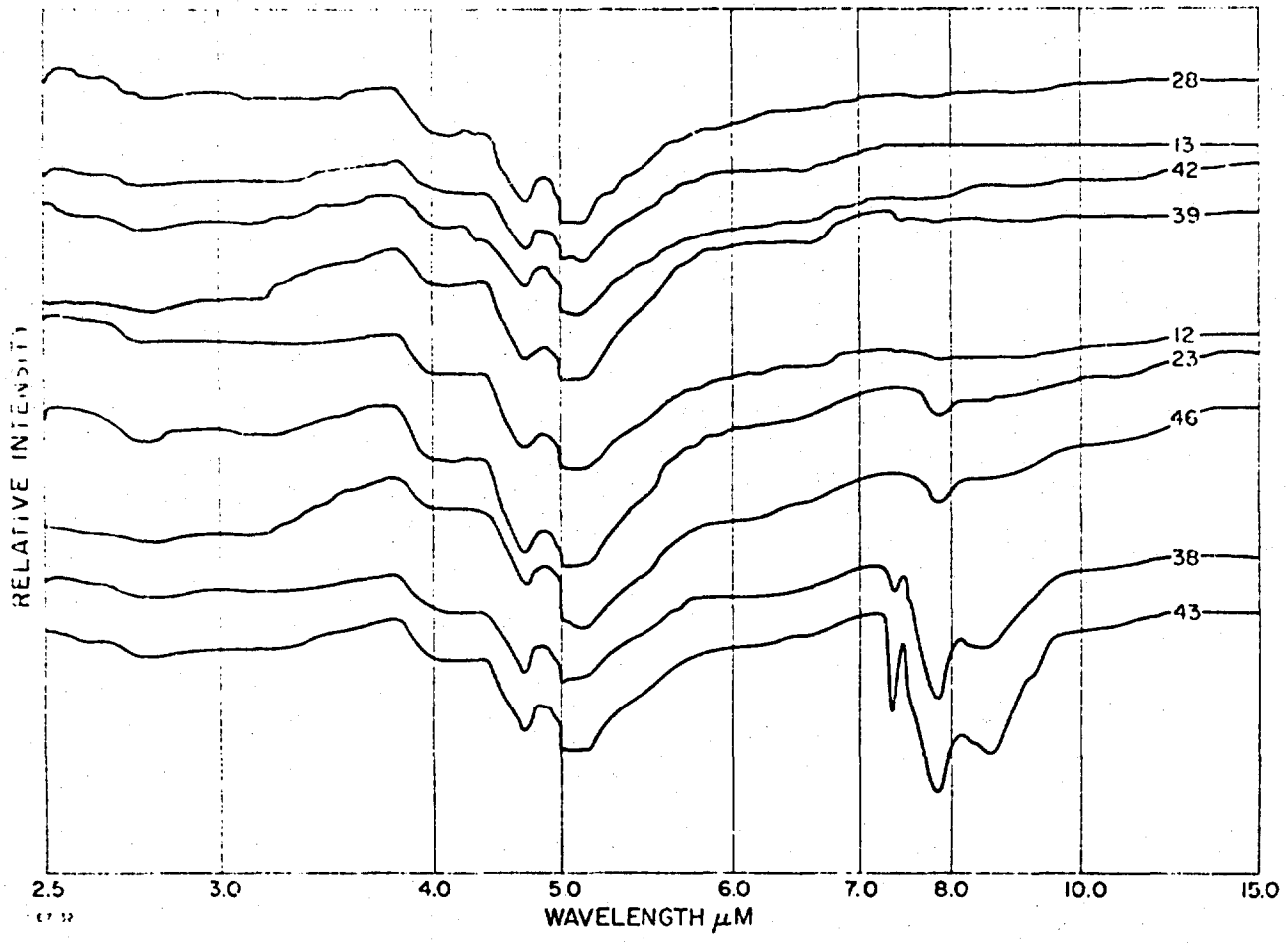

Figure 2. IR absorption spectrum of representative diamond discs.

All of the diamonds were transparent at 12.5 μm. The spectra have been characterized by a relative absorption $A_{7.9}$ which compares the transmission at 7.9 μm to the transmission at 12.5 μm as read from the spectrogram.

$$A_{7.9} = 1 - (I_{7.9}/I_{12.5}) \qquad (2)$$

The values of $A_{7.9}$ are given in Table I, column 4.

The correlation between the absorption at .25 μm and at 7.9 μm is presented in Figure 3. Here, the circles represent the individual diamond numbers and the relative absorption values are cross plotted. One sees that those diamonds with low values of $A_{.25}$, namely diamond number 13, 28, 39 and 42, also have low values of $A_{7.9}$. Presumably these are Type II diamonds and should also have low values of β. There is a group of diamonds with values of $A_{7.9}$ only slightly higher than the aforementioned four which have higher values of $A_{.25}$. Finally there is a very large group of diamonds with high values of absorption at both wavelengths. These latter are very likely to be Type I diamonds.

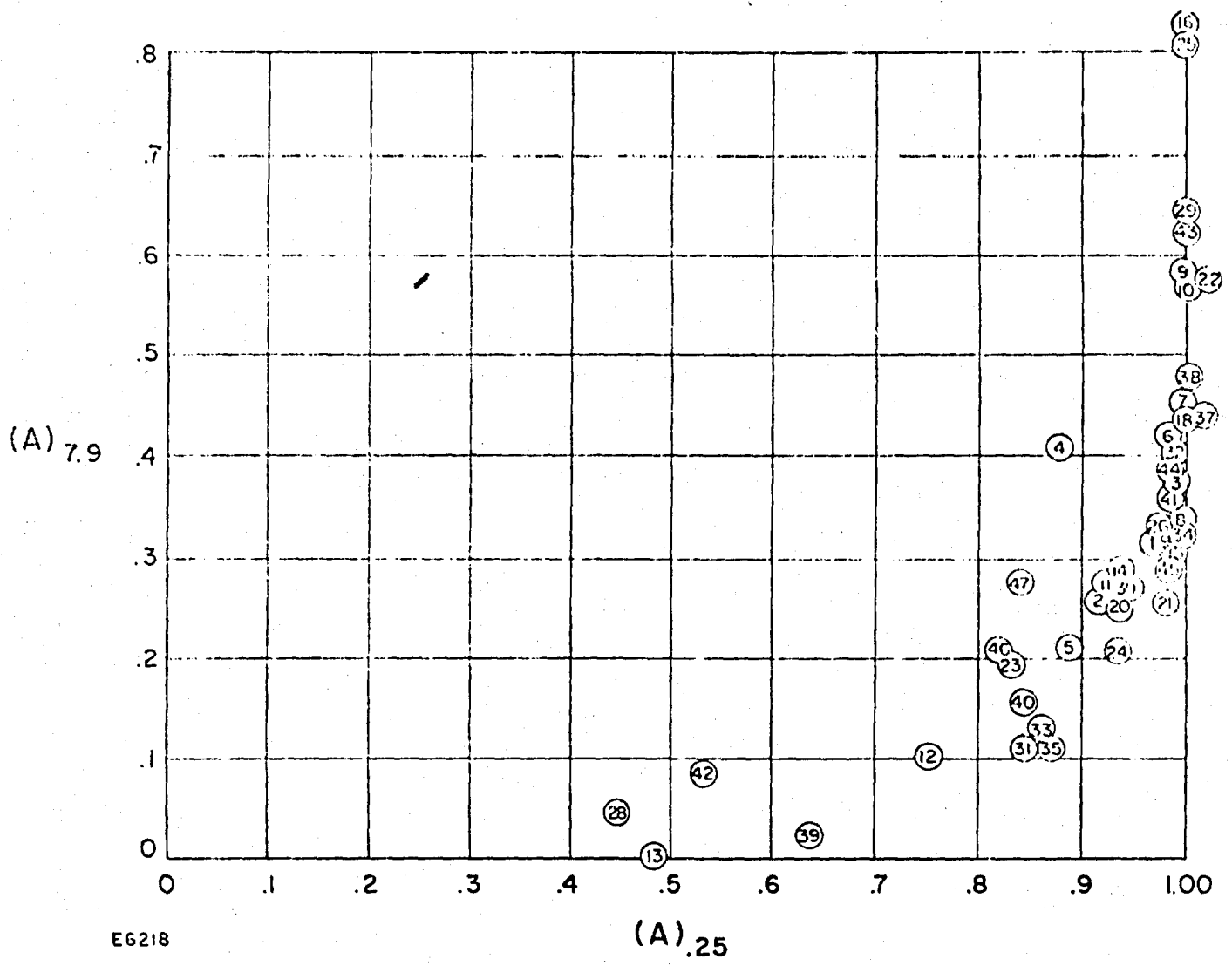

Figure 3. Correlation between absorption at 7.9 μm and .25 μm for 47 natural diamonds.

IV. DIRECT ABSORPTION MEASUREMENTS

The diamonds that were chosen for a direct determination of β at 10.6 μm were all of those with low and intermediate values of $A_{.25}$ and some of those with a high absorption. Thus, the distribution of βs could be obtained to reveal whether the transparency to the .25 μm mercury line is correlated with β.

The experiment consisted in passing a focused 10.6 μm laser beam through the diamond, measuring the incident and transmitted intensity and the heating resulting from absorption. The diamonds were sufficiently parallel across the small irradiated spot diameter so that internal reflection would interfer to an unknown degree with the transmitted beam. A correction was therefore applied to the measurements to give corrected values of β. Details of how this was done are given in Appendix A.

The laser beam was approximately 20 watts, obtained from a Perkin Elmer Model 6200 CO_2 laser. A collimated beam, 1.3 cm diameter was sharply focused through the diamond with a copper mirror of 10 cm focal length. Approximately 12% of the laser power was transmitted through a hole in the mirror into a differential thermocouple calorimeter so that the laser power could be monitored. After passing through the diamond, the energy was received on a calibrated absorber and integrated. The temperature rise of the absorber was recorded and converted to the transmitted beam intensity. For the incident beam intensity, the diamond was removed from the sample holder and the transmitted beam measured directly. The specimens were clamped between two thin copper discs having a hole for transmission of the laser beam. A copper-constantan thermocouple was attached to the holder. Absorption of energy by the diamond was transmitted to the holder and the temperature recorded. The weight of the copper diamond holder was .59g. Its heat capacity was .23J/^{o}C. The heat capacity of an average size diamond was .0036J/^{o}C.

A correction is needed for the amount of energy that was intercepted by the diamond holder from fringes of the laser beam. Therefore, a calibration run was made in which the heating of the holder alone was measured as a function of the exposure time. This was not linear with time because the diamond holder was constructed of a number of materials, copper, stainless steel, phenolic, etc., each with a different thermal diffusivity. The exposure time for various diamonds was also different. Those with the highest absorption coefficient were given short exposures to prevent overheating and those with low absorption were exposed for longer times.

The power absorbed by the holder alone was about .08 watts. This was substracted from the power absorbed by the diamond plus holder to give the absorption of the diamond alone. This correction was usually quite small. For example, the diamond #28 which had the lowest value of β plus the holder absorbed .202 watts and diamond #13 plus the holder absorbed .224 watts.

The results of the direct absorption experiment are also shown in Table I, columns 5 thru 11. Column 5 is the exposure time, 6 gives the incident laser power; column 7 is the transmitted power; column 8 is the temperature rise of the diamond and holder; column 9 is the power absorbed in the diamond alone. Column 10 is the value of β obtained without correction for interference between the transmitted and internally reflected beam. Column 11 is the value of β obtained after correction for this effect. The values of β are plotted against the relative absorption in the infrared, $A_{7.9}$ in Figure 4 and against the relative absorption in the ultraviolet $A_{.25}$ in Figure 5. Note that the scattering in the data is amplified by the use of a logarithmic plot. The lowest value of β that has been observed is .021 for diamond No. 28.

The data shows that $A_{.25}$ is a rough guide to the value of β but it is not quantitatively reliable. For example diamonds No. 28 and 13 have similar values of $A_{.25}$ but a factor 3 difference in β.

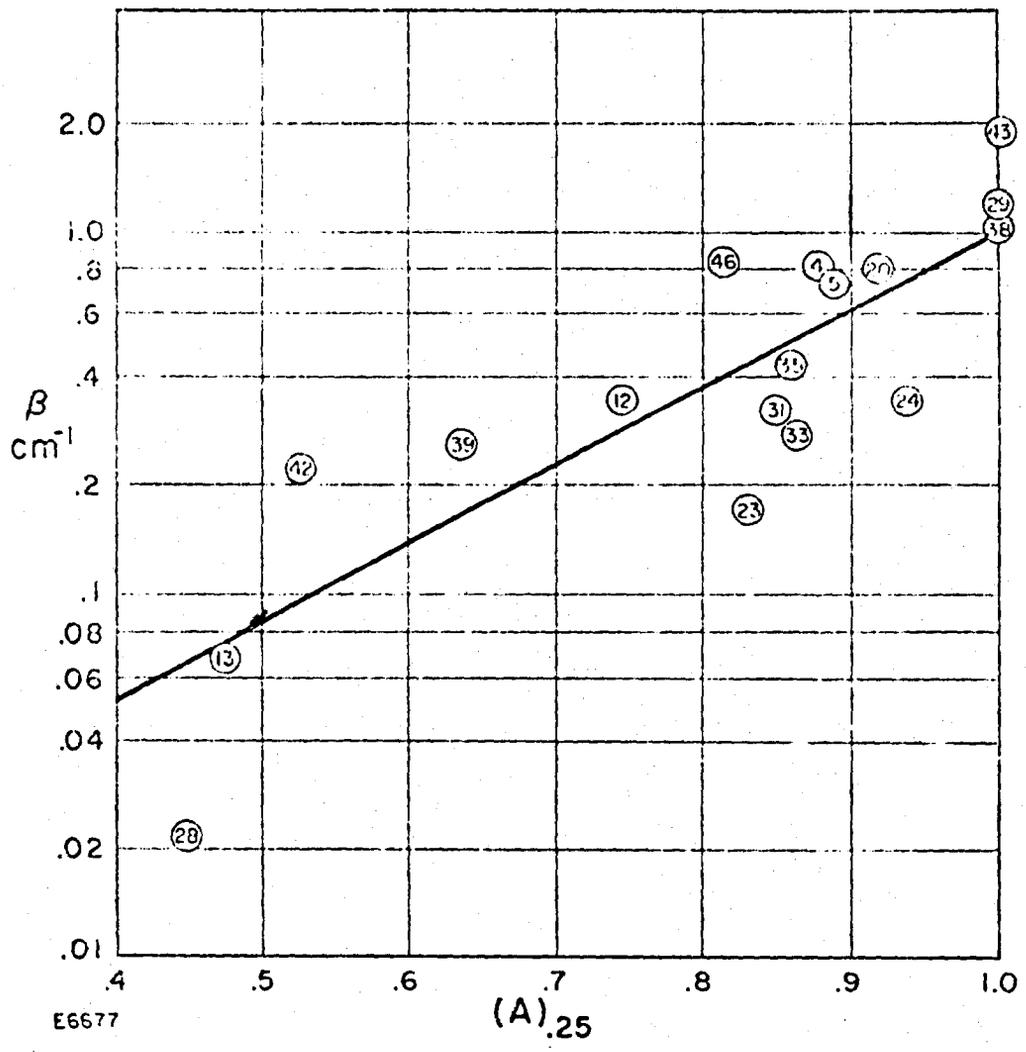

Figure 4. Distribution of absorption coefficient, β versus absorption at .25 μm for Type I and Type II diamonds.

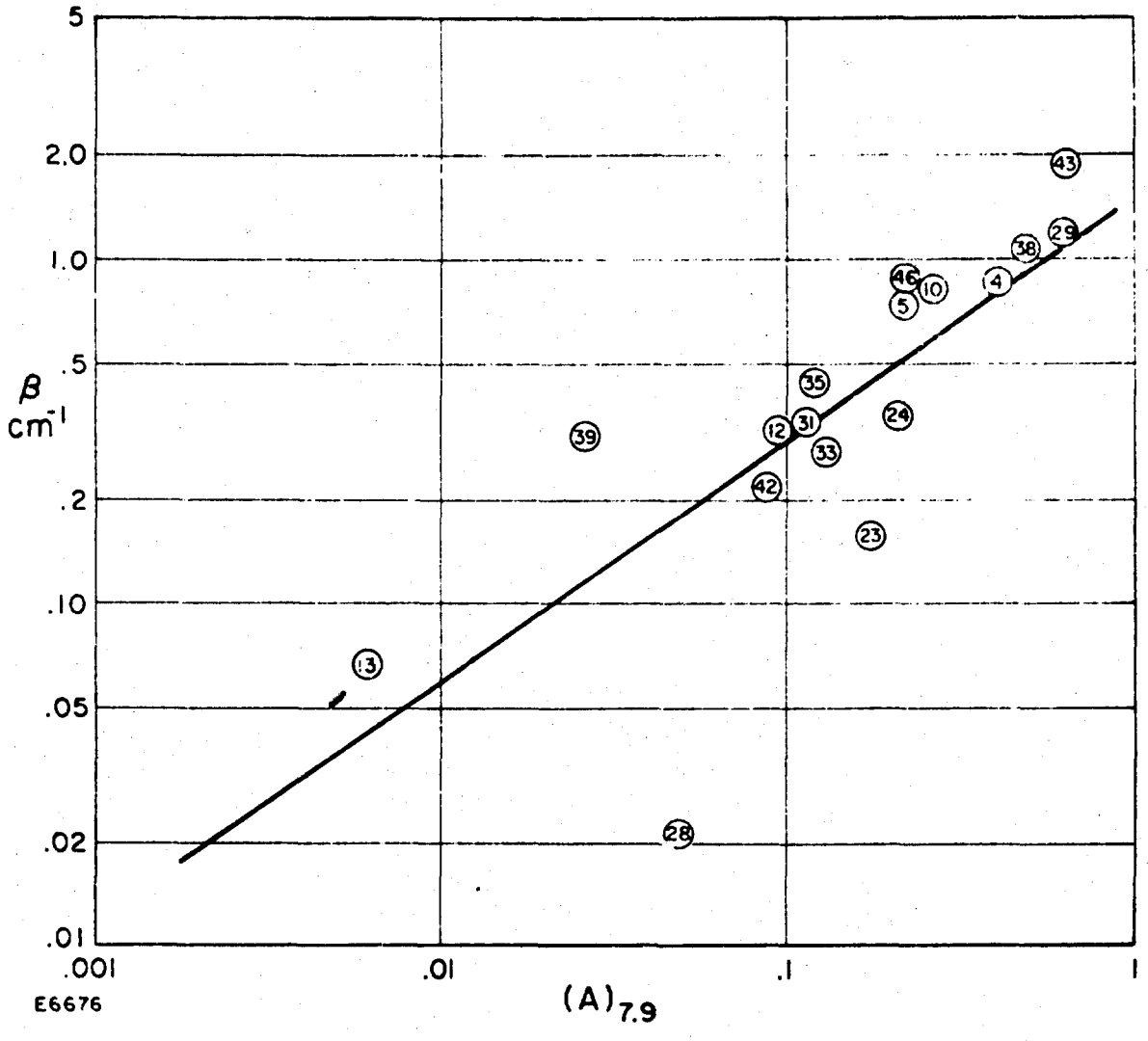

Figure 5 Distribution of absorption coefficient, β versus absorption at 7.9 μm for Type I and Type II diamonds.

Approximately 20% of the diamonds have values of β less than .5, however, if a selection had been made of those diamonds with values of $A_{.25} \leq .75$, only half of the low β diamonds would have been found. The conclusion of this spectroscopic study is that if diamonds show a high absorption in the ultraviolet, they also have a high absorption at 10.6μm. If they show a high transparency in the ultraviolet, they also have a low absorption at 10.6μm. However, there are a number of diamonds for which the ultraviolet spectrum is an unreliable guide to the 10.6μm absorption.

V. DESIGN OF DIAMOND HOLDER

Figures 4 and 5 show that we can expect to find diamonds for windows with $\beta \leq .5\ cm^{-1}$. The diamond cutters say that they may have difficulty in cutting plates thinner than 2mm because of the danger of cracking. We may therefore expect an absorption by the window of 6% or less of the transmitted power. The diamond temperature may not exceed 800°C, the temperature at which transition to diamond becomes accelerated. The transmitted power therefore depends on the efficiency of cooling of the window that can be provided.

A water cooled window holder has been designed in which the diamond is clamped at the edges of its parallel faces between two water cooled copper discs. This is shown in Figure 6. A small hole in the center allows the laser beam to be transmitted through the diamond. Thin annular gold washers distribute the clamping force uniformly to the window surface. Water flowing at high velocity is brought into contact with the edge of the diamond by constructing the holder in the shape of a nozzle with the window located at the smallest cross section. In addition to high coolant velocity, the diamond holder introduces swirl to further improve heat transfer. It is estimated that a Reynolds Number of about 40,000 will be reached by the water flowing over the diamond surface. The expected heat transfer coefficient will be about 6.7 watts/cm^2 deg. If we allow the diamond temperature rise to be 600°C, the heat transfer to water will be 1500 watts. For an absorption of .06, the transmitted laser power may be 25 kW. In addition to the heat transfer to the water, there is also conduction heat transfer to the cooled metal surfaces that clamp the edge of the diamond. However, in this case, the heat must be transferred through metal interfaces. According to McAdams[3] the contact coefficient for heat transfer between machined surfaces under moderate pressure is $h_c = 1.7$. In our diamond holder, there are two such surfaces in series

[3] W. H. McAdams, Heat Transmission, McGraw Hill (1954).

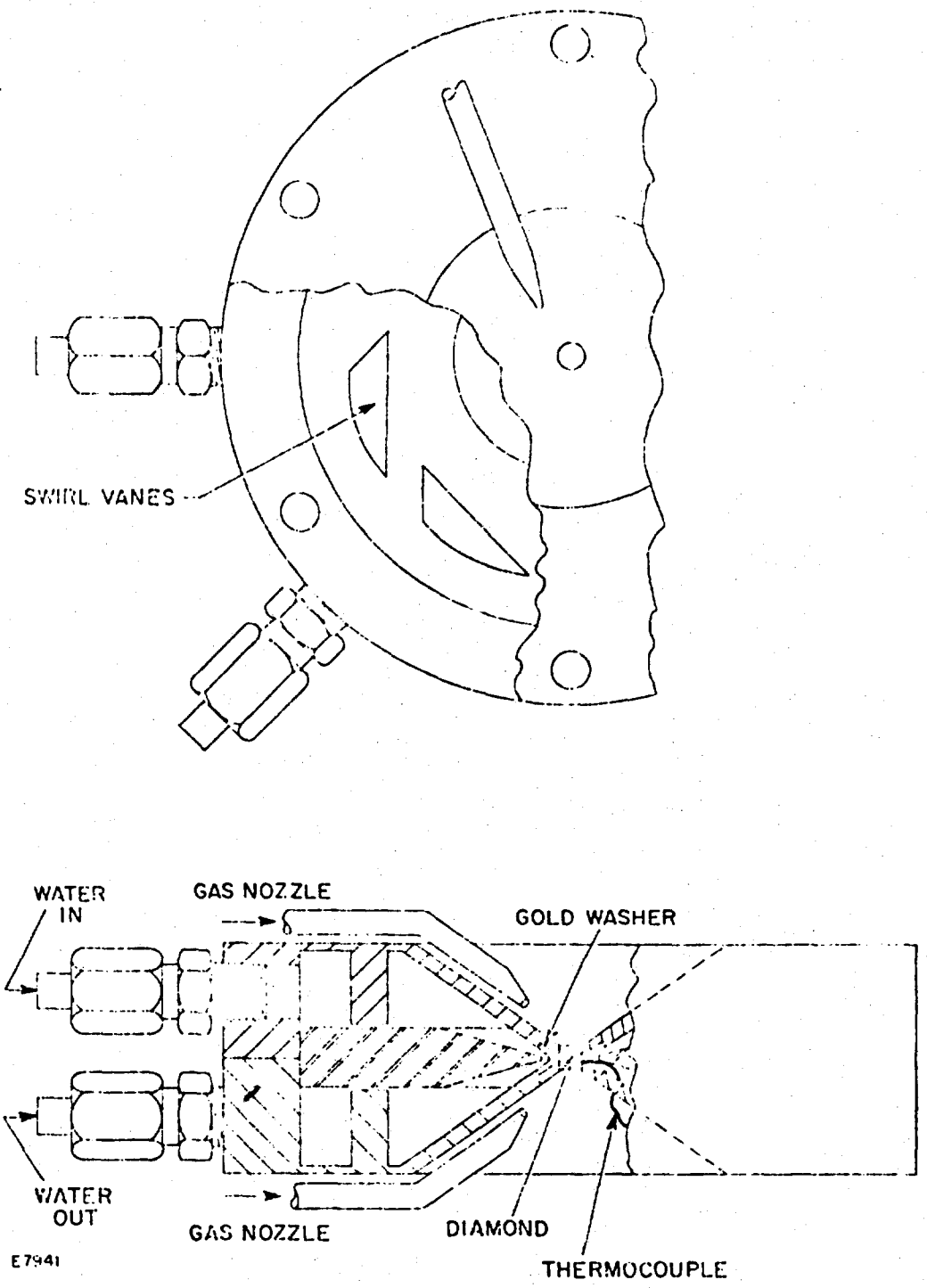

Figure 6. Water cooled diamond window and window holder.

and two in parallel giving 1.7 as an estimate of the resultant conduction heat transfer coefficient. The clamped surface will have about the same area as the water cooled surface, therefore, it is estimated that the conduction heat removal will only be about 25% of the heat transferred directly to water at the edge of the window. This 25% additional margin is more than sufficient to compensate for another source of temperature to be discussed next.

In addition to the ΔT at the surface, there is also a radial temperature distribution $\Delta T(r)$ due to the heat conduction within the diamond. The maximum value of $\Delta T(r)$ depends on the distribution of laser flux. It is clear that the smaller the spot diameter, the larger will be the conduction ΔT. For a focal spot of .2 cm radius, the central temperature rise is about $35^{\circ}C$ or about 7% of that at the surface. The conclusions of these estimates is that it should be easy to transmit the laser beam from our 15 kW HPL industrial laser through a diamond window. Additional information on the diamonds and the window holder will be contained in the report for the next period.

VI. EXPERIMENTS WITH CaF_2 WINDOW MATERIAL

Toward the end of the present reporting period, an opportunity was presented to us to subject two samples of calcium fluride to a pulsed laser beam from an AERL, Inc. H-F combustion laser (λ = 2.8μm). This laser had reached an optical pulse energy of 60 J for 5 μseconds under the best operating conditions[4].

One of the experiments that was planned was to substitute deuterium for the hydrogen to test windows with a D-F pulse (3.8 μm). However, this procedure was not successful. For an unknown reason, the laser did not perform well with deuterium. Hydrogen was then used and pulses of 23 J, were obtained at the time of the experiments to be described. The energy transmitted to the CaF_2 was a focused beam of 20J, 5 μsecond long. The remainder of the energy was absorbed in a calorimeter used to measure the beam power. The target specimens were single crystal CaF_2 and pressure induced recrystalized CaF_2. These were supplied to us by AFCRL as plane polished prisms. The laser beam from the HF laser was twice reflected from copper mirrors with 25 cm focal length. This produced a rectangular focal spot .2 by .3 cm as determined by making preliminary burns on an absorbing target. Before reflection from the mirrors for focussing, 13% of the energy was diverted to a calorimeter by a saphire beam splitter. The remaining energy was brought to a focus with an estimated intensity of 6.7×10^7 watt/cm^2 (330 J/cm^2).

---

(4) The development of this laser was partly funded by the Air Force and partly by AERL, Inc. IRAD. For a description, see R. Limpaecher, H. L. Chen, and J. Daugherty, Development of HF-DF Pulsed Chemical Laser. Final Report for AFWL Contract F29601-73-C-0122 to be published.

The radiation produced no visible damage to the windows, nor was any damage expected. The stress level that was believed to be induced in the target as a result of these pulses is calculated by the method described in Appendix B.

It is shown there that the peak stress induced by a short laser pulse of energy J_p and spot diameter d_s in passing through a window is

$$\sigma_p = \sqrt{2}\ \alpha E\ T_o\ J_p/2\ d_s^2 \qquad (3)$$

This is evaluated for CaF_2 by using $\alpha = 19.7 \times 10^{-6}\ K^{-1}$ for the expansion coefficient, $E = 7.58 \times 10^{11}\ d/cm^2$ for the modulus of elasticity; and $T_o = 1.88 \times 10^{-3}\ cm^2\ K/J$ for a characteristic constant appropriate to CaF_2 having an absorption coefficient $\beta = .004\ cm^{-1}$. The result is

$$\sigma_p = 2.0 \times 10^4\ J_p/d_s^2\ d/cm^2 \qquad (4)$$

In the present experiment J_p was 20 Joules and the measured spot size was .2 x .3 cm. This gives a peak principle stress of $1.0 \times 10^7\ d/cm^2$. The yield strength of CaF_2 crystals is given in handbooks as $3.7 \times 10^8\ d/cm^2$. Therefore we did not anticipate that the crystals would be damaged from the transmission of these pulses.

Development work on this laser will hopefully continue and it may be possible to do additional testings with more energy on a smaller spot size.

VII. CONCLUSIONS

The laser window test facility should be available shortly for subjecting various types of window material to high intensity CW and pulsed laser beams. Distortion or lensing of the window will be observed by interferometry and other effects observed by temperature rise or stress measurement.

Among the first windows to be tested will be Type II diamond plates. In selecting stones for use in making the windows, ultraviolet absorption spectroscopy is a useful guide although this may lead to overlooking of some useful diamonds. However, even if the absorption coefficient is as high as .3 cm^{-1}, it should still be possible to make a window that will pass 15 kW of CW laser radiation power without damage. Additional IR absorption spectroscopy will be useful also. In the next reporting period, we expect to have tests on some diamond windows and also some windows of other materials.

ACKNOWLEDGMENT

The author wishes to thank R. Limpaecher for making available the H-F laser; also H. Posen and Major C. Collins of AFCRL for supplying the samples of CaF_2 window. The absorptions spectra of the forty-seven diamond specimens was obtained by R. Harned.

APPENDIX A
CORRECTION OF β FOR INTERNAL REFLECTION

This theory is based on the treatment in Born and Wolf[5] for the transmission of a plane electromagnetic wave through a dielectric plate having parallel faces. Let n' be the refractive index of the plate and n that of the surrounding medium.

The following uncorrected quantities are experimentally measured:

I = Incident Intensity = $A(i)\,A^{*}(i)$. This is measured with a calorimeter located behind the aperture in the sample holder and with no specimen in the holder. Here A(i) is the amplitude of the electric field of the incident wave.

$I\mathcal{J}_{eff}$ = Transmitted Power. This is measured in the same way as I except that there is now a dielectric plate in the holder.

$I\mathcal{A}_{eff}$ = Absorbed Power. This is determined by measuring the temperature rise of the plate, plus holder and then subtracting the temperature rise of the holder alone.

$$I\mathcal{A}_{eff} = (c_p m \Delta T/\tau)_{\text{sample + holder}} - \text{same quantity for holder alone} \qquad \text{(A1)}$$

where c_p is the specific heat
m is the mass
ΔT is the temperature rise and
τ is the exposure time.

(5) Born, M., and Wolf, E., Principles of Optics, Pergamon Press (1970) p. 323 ff.

Let $1-\eta^{\frac{1}{2}}$ be the fraction of the amplitude that is absorbed by the plate in a single pass. $(1-\eta)$ is the single pass absorption of the wave intensity. It is related to the absorption coefficient β for small values of β by

$$\eta = \exp(-\beta d) \approx 1 - \beta d \tag{A2}$$

where d is the plate thickness. Also, let $\delta/2$ be an arbitrary phase change of the amplitude in a single passage through the plate.

Furthermore, following the notation in Born and Wolf, let r and t be the reflection coefficient and transmission coefficient for the amplitude of a wave striking the plate from the surrounding medium; and r' and t' be the same quantities for the amplitude of a wave inside the plate. These are related to the reflectivity of the plate, $\mathcal{R}$ and its transmissivity $\mathcal{T}$ for single passes of radiation

$$\mathcal{R} = -r\,r' = \left(\frac{n' - n}{n' + n}\right)^2 \tag{A3}$$

$$\mathcal{T} = t\,t' = \frac{4n'}{(n' + n)^2} \tag{A4}$$

$$\mathcal{R} + \mathcal{T} = 1 \tag{A5}$$

The problem is to find η by using the measured quanties $\mathcal{T}_{eff}$ and $\mathcal{R}_{eff}$.

The reflected amplitude from a plate with multiple internal reflections is given by

$$\begin{aligned} A(r) &= A(i)\left[r + r'tt'\,\eta\, e^{i\delta}\,(1 + r'^2\,\eta\, e^{i\delta} + r'^4\,\eta^2\, e^{2i\delta} + \ldots.)\right] \\ &= A(i)\left[r + \eta\, r'\, tt'\, e^{i\delta}/(1 - \eta\, r'^2\, e^{i\delta})\right] \end{aligned} \tag{A6}$$

Using $r = -r'$ and (A3) to (A5) we have

$$A(r) = -A(i)\sqrt{\mathcal{R}}\ (1-\eta\ e^{i\delta})/(1-\eta\ \mathcal{R}\ e^{i\delta}) \tag{A7}$$

The reflected intensity = $A(r)\ A^{*}(r)$. The reflectivity $\mathcal{R}_{eff} = A(r)\ A^{*}(r)/A(i)\ A^{*}(i)$

$$\mathcal{R}_{eff} = \mathcal{R}(1+\eta^{2}-2\eta\cos\delta)/(1+\eta^{2}\mathcal{R}^{2}-2\eta\,\mathcal{R}\cos\delta)$$

$$\mathcal{R}_{eff} = \mathcal{R}\ \frac{(1-\eta)^{2}+4\eta\sin^{2}\delta/2}{(1-\eta\mathcal{R})^{2}+4\eta\,\mathcal{R}\sin^{2}\delta/2} \tag{A8}$$

In a similar manner, the transmitted amplitude and intensity is obtained for multiple internal reflections.

$$A(t) = A(i)tt'\left[\eta^{\frac{1}{2}} + r'^{2}\,\eta^{\frac{3}{2}}\,e^{i\delta} + r'^{4}\,\eta^{\frac{5}{2}}\,e^{2i\delta} + \ldots.\right]$$

$$= A(i)tt'\ \eta^{\frac{1}{2}}/(1 - r'^{2}\,\eta\,e^{i\delta})$$

$$= A(i)\ \mathcal{T}\ \eta^{\frac{1}{2}}\ /(1 - \mathcal{R}\,\eta\,e^{i\delta}) \tag{A9}$$

The transmitted intensity = $A(t)\ A^{*}(t)$
The transmissivity $\mathcal{T}_{eff} = A(t)\ A^{*}(t)/A(i)\ A^{*}(i)$

$$\mathcal{T}_{eff} = \mathcal{T}^{2}\ \eta/(1+\mathcal{R}^{2}\eta^{2} - 2\mathcal{R}\eta\cos\delta)$$

$$\mathcal{T}_{eff} = \frac{\mathcal{T}^{2}\eta}{(1-\mathcal{R}\eta)^{2}+4\mathcal{R}\eta\sin^{2}\delta/2} \tag{A10}$$

We now eliminate δ by a change in variable. Let

$$\chi = \eta \sin^2 \delta/2 \tag{A11}$$

and substitute in (A10)

$$\chi = \left[\mathcal{J}^2\eta - \mathcal{J}_{eff}(1-\mathcal{R}\eta)^2\right]/4\mathcal{J}_{eff}\mathcal{R} \tag{A12}$$

This is now used in (A8)

$$\mathcal{R}_{eff} = (\mathcal{J}_{eff} + \eta\mathcal{J} + \eta^2\mathcal{R}\mathcal{J}_{eff})/\eta\mathcal{J} \tag{A13}$$

This maybe solved for η from the quadratic

$$\eta^2\mathcal{R}\mathcal{J}_{eff} + \eta\mathcal{J}(1-\mathcal{R}_{eff}) - \mathcal{J}_{eff} = 0 \tag{A14}$$

For diamond, n' = 2.415, $\mathcal{R}$ = .1717 and $\mathcal{J}$ = .8283. See (A3) and (A4). $\mathcal{R}_{eff}$ can be obtained from the measured value of $\mathcal{A}_{eff}$ by

$$\mathcal{J}_{eff} + \mathcal{R}_{eff} + \mathcal{A}_{eff} = 1 \tag{A15}$$

Finally the value of β is obtained from (A2). The results of this calculations are given in Table I.

APPENDIX B
WINDOW STRESS FROM FOCUSSED LASER BEAM

Consider a laser beam of pulse energy J_p and pulse duration t_p. It is focussed through a window of diameter 2b and the irradiated area has a diameter d_s. (For a multimode laser, d_s may be many times larger than the diffraction limited spot size). The window has a thickness t and an absorption coefficient β, so that the energy deposited in the window during the pulse is

$$Q_w = J_p \left[1-\exp(-\beta t)\right] \tag{B1}$$

The distance r_d that a heat pulse diffuses is

$$r_d = \sqrt{xt_p} \tag{B2}$$

where x is the diffusivity (=.0293 for CaF_2). Depending on the pulse duration, the heat may be confined to the initial zone, d_s, or it may diffuse to a larger zone of diameter $2r_d$. For the CaF_2 window, it is known that d_2 is much larger than $2r_d$. Therefore, the temperature distribution is the same as the intensity distribution, $I_p(r)$. Note that T(r) is independent of the window thickness.

$$T(r) = \beta I_p(r) t_p / \rho C_p \quad \text{deg K} \tag{B3}$$

The equation for radial stress σ_r and tangential stress σ_θ in a thin circular disc with temperature symmetrical about r = 0 is given by[6]

$$\frac{d\sigma_r}{dr} + \frac{\sigma_r - \sigma_\theta}{r} = 0 \tag{B4}$$

---

(6) Timoshenko and Goodier, Theory of Elasticity, McGraw Hill, (1951) p.406

There is no shear stress because of radial symmetry. The components of strain are given by

$$\epsilon_r - \alpha T = \frac{1}{E}(\sigma_r - \nu\sigma_\theta)$$
$$\epsilon_\theta - \alpha T = \frac{1}{E}(\sigma_\theta - \nu\sigma_r) \tag{B5}$$

where α is the coefficient of linear expansion and ν is Poisson's ratio. The differential equation may be integrated by noting that for an isotropic material,

$$\epsilon_r = \frac{d}{dr}(r\epsilon_\theta) \tag{B6}$$

This gives

$$\sigma_r = -\frac{\alpha E}{r^2}\int_0^r Trdr + \frac{E}{1-\nu^2}\left[C_1(1+\nu) - C_2(1-\nu)\frac{1}{r^2}\right]$$

$$\sigma_\theta = \frac{\alpha E}{r^2}\int_0^r Trdr - \alpha ET + \frac{E}{1-\nu^2}\left[C_1(1+\nu) + C_2(1-\nu)\frac{1}{r^2}\right]$$

C_2 must be zero in order for ϵ_θ to be zero at the origin. At the edge where r = b, we must have $\sigma_r = 0$. Therefore

$$C_1 = (1-\nu)\frac{\alpha}{b^2}\int_0^b Trdr$$

The final equations for the stress in a thin isotropic plate

$$\sigma_r = \alpha E\left[\frac{1}{b^2}\int_0^b Trdr - \frac{1}{r^2}\int_0^r Trdr\right]$$
$$\sigma_\theta = \alpha E\left[-T + \frac{1}{b^2}\int_0^b Trdr + \frac{1}{r^2}\int_0^r Trdr\right] \tag{B7}$$

We believe that for the H-F laser, I_p has a flat topped distribution.

$$I_p = 4 J_p/\pi t_p d_s^2 \ W/cm^2$$

$$\text{for } 0 \leq 2r \leq d_s$$

$$I_p = 0 \text{ for } 2r > d_s \tag{B8}$$

On substituting in (B3) it follows that

$$T = T_o J_p/d_s^2 \text{ for } 0 \leq {}^2r \leq d_s$$

$$= 0 \qquad \text{for} \qquad {}^2r > d_s \tag{B9}$$

where $T_o = 4\beta/\pi\rho c_p$

Using $\beta = .004\ cm^{-1}$ and $\rho c_p = 2.71\ J/cm^3\ K$ for CaF_2, $T_o = 1.88 \times 10^{-3}\ cm^2\ K/J$. On substituting this result in (B7) we find that for short, flat topped laser pulses,

$$\sigma_r = \alpha E T_o J_p/2d_s^2 \text{ for } 2r \leq d_s$$

$$\sigma_r = (\alpha E T_o J_p/8)\left(\frac{1}{b^2} - \frac{1}{r^2}\right) \text{ for } 2r > d_s \tag{B10}$$

The radial stress is in compression. It is proportional to the beam intensity and is constant within the irradiated region, decreasing as $1/r^2$ to zero at the boundary

$$\sigma_\theta = \sigma_r \text{ for } 2r \leq d_s$$

$$\sigma_\theta = (\alpha E T_o J_p/8)\left(\frac{1}{b^2} + \frac{1}{r^2}\right) \text{ for } 2r > d_s \tag{B11}$$

The tangential stress reverses from compression inside the irradiated spot to tension outside and then becomes weaker as one moves toward the edge of the window.

The peak principal stress is

$$\sigma_P = \sqrt{2}\, \alpha E\, T_o\, J_p / 2 d_s^2 \qquad \text{(B12)}$$

It is in compression inside the irradiated spot and reverses to the same magnitude of tension at the spot boundary.